

# REVALIDATION OF THE HUYGENS DESCENT CONTROL SUB-SYSTEM

J.C. Underwood, J.S. Lingard and M.G. Darley

*Vorticity Ltd., Chalgrove, Oxfordshire OX44 7RW, United Kingdom*

## ABSTRACT

The Huygens probe, part of the Cassini mission to Saturn, is designed to investigate the atmosphere of Titan, Saturn's largest moon. The passage of the probe through the atmosphere is controlled by the Descent Control Sub-System (DCSS), which consists of three parachutes and associated mechanisms.

The Cassini / Huygens mission was launched in October 1997 and was designed during the early 1990's. During the time since the design and launch, analysis capabilities have improved significantly, knowledge of the Titan environment has improved and the baseline mission has been modified. Consequently, a study was performed to revalidate the DCSS design against the current predictions.

## Nomenclature

$a_{11}$	Added mass (kg)
$C_D$	Drag coefficient
$C_{mq}$	Pitch damping coefficient
$D_p$	Projected diameter
$g$	Acceleration due to gravity ( $m/s^2$ )
$m_s$	System mass (kg)
$S_p$	Projected Area ( $m^2$ )
$V$	Velocity (m/s)
$\rho$	Density ( $kg/m^3$ )

## 1 INTRODUCTION

In the 10 years since the DCSS was designed much has changed: the knowledge of the Titan atmosphere has improved, parachute inflation analysis tools have been refined and the entry conditions of the probe into the Titan atmosphere have been revised.

As the release of Huygens from Cassini approaches, this is the last opportunity to revalidate the design of the Huygens probe using the latest information gained from Cassini and predict the performance we expect on 14<sup>th</sup> January 2005.

## 2 SEQUENCE

The Huygens DCSS sequence starts at a nominal Mach number of 1.5, 157 km above the surface of Titan (Fig 1a). At this point, approximately 260 seconds after first encountering the atmosphere, the probe is still encased in its protective aeroshell. The first function of the DCSS is to remove the rear portion of the aeroshell using a mortar deployed, 2.59 m Disk-Gap-Band

(DGB) parachute of a similar design to that used on Viking (Fig 1b).

As the pilot chute separates the rear aeroshell from the probe (Fig 1c), a second, 8.3 m parachute is deployed by a lanyard. This parachute, a DGB of a slightly different design, provides stability as the probe decelerates through Mach 1 (Fig 1d) and sufficient drag to allow the front aeroshell to fall away from the probe when it is released 32.5 seconds into the sequence (Fig 1e).

Once the aeroshell has separated from the probe, the science instruments start to take data as the probe descends through the upper atmosphere (Fig 1f).

If the probe were to remain in this configuration the probe descent to the surface would take over 5 hours. Since the Cassini orbiter is only visible for 2.5 hours, the main parachute must be released 15 minutes after the start of the descent sequence by means of three pyrotechnic cutters and a 3.03 m stabilising drogue deployed (Fig 1g).

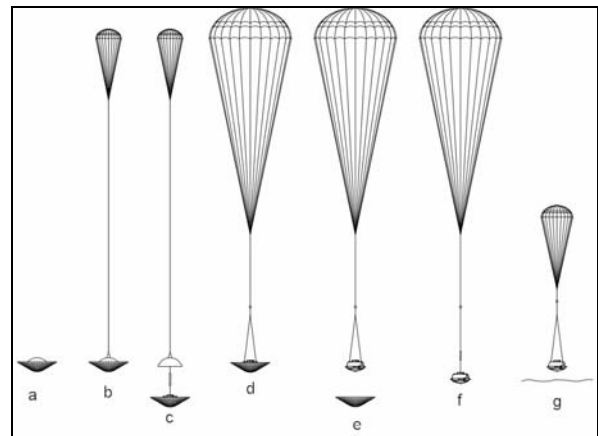


Fig. 1 Probe Sequence

The sequence has been documented in detail elsewhere [1].

## 3 CHANGES

### 3.1 Atmospheres

In order to design the Huygens probe, assumptions had to be made about the environment it would experience on arrival at Titan. The most crucial of these related to the atmosphere. Its temperature and density profiles determine the overall trajectory and the conditions at initiation of the descent sequence whilst its

composition is critical for the design of the heat shield used to protect the probe during the initial entry into the atmosphere.

The original 1987 Lellouche-Hunten atmosphere model [2] defined three profiles (minimal, nominal and maximal) and was used throughout the development of the Huygens DCSS. This was superseded by a new model [3] derived by Yelle in 1994. However, since the DCSS was already designed and tested it was not fully revalidated against the new atmosphere.

Subsequently, the atmosphere was modified by the addition of coherent gravity waves [4] which could be adjusted to give a worst case atmosphere and an alternative atmosphere, TitanGRAM, was produced independently [5] which generates random perturbations which are more suited to Monte-Carlo analysis. Both use the Yelle values as their nominal profiles.

Over the next few months it is expected that these models will be further refined using data from Cassini's targeted flybys of Titan in October 2004 and December 2004

### 3.2 Initial Conditions

During the design of Huygens the responsibility for trajectory analysis was split between the prime contractor (Entry phase) and the DCSS contractor (Descent phase). This split made it impossible to carry out large numbers of simulations from the atmosphere interface to the surface. In order to design the DCSS, seven design cases were defined which gave extreme conditions at initiation. These were derived using the extreme cases tabulated below.

Table 1. Design Initiation Cases

Condition	Entry Angle	Atmos	Mass	T0
Nominal	Nom	Nom	Nom	Nom
Min Mach	Steep	Min	Max	Late
Max Mach	Shallow	Max	Min	Early
Max q	Steep	Min	Max	Early
Min q	Shallow	Max	Min	Late
Failure Max q	Steep	Min	Max	FoA
Failure Max Mach	Shallow	Max	Min	FoA

These seven cases were derived from three trajectories: nominal, steep entry and shallow entry. Three points were generated on each trajectory representing the earliest nominal initiation (based on sensing uncertainty), latest nominal initiation and fire on arm (FoA) – a single failure case.

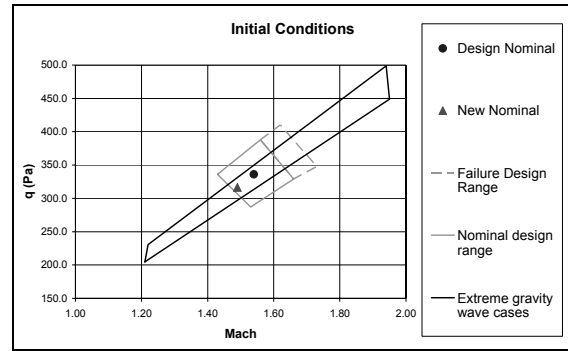


Fig. 2. Revised initial conditions

As a result of the change of atmosphere model and a change in entry angle brought about by a change in the Cassini / Huygens geometry during the mission, the entry trajectory and thus DCSS initiation points changed. New initiation cases were derived using trajectories modelled with the new atmosphere and entry conditions. Since the effects of gravity waves on the sequence sensing logic are not straightforward, a number of cases were examined in order to determine the worst case conditions. The new envelope is shown graphically in Fig. 2.

It should be noted that the new analysis takes account of failure cases which were not considered during the design of the DCSS. This explains in part the large increase in the range of initial conditions.

It can be seen that the ranges of Mach number and dynamic pressure at DCSS initiation have increased significantly from those it was designed for. The new analysis used only five initial conditions (one nominal and four worst cases), the high Mach and high q non-failure cases were discarded since they were enveloped by the other four cases.

### 3.3 Masses

During development all modelling was performed using the extreme design range of masses, including margins. During the final integration of the probe all items were weighed, so the "as flown" masses are now available to refine the predicted performance. The only remaining mass uncertainty is the loss from the aeroshell during entry.

### 3.4 Aerodynamic Databases

Since the completion of the development programme, data obtained during the programme and on other subsequent programmes have allowed refinement of the aerodynamic databases for the probe and parachutes. The current study provided an opportunity to incorporate these data into the analyses.

## 4 THE TOOLS

### 4.1 Timeline and deployments

Originally, the overall descent timeline, deployments and parachute inflation loads were each modelled using separate, dedicated software. For the early stages of the re-validation new models were written and validated against output from the original software. However, although this approach was adequate for checking a small number of design cases, it was inadequate for running Monte-Carlo entry and descent simulations.

### 4.2 Inflations

Parachute inflations were modelled using an engineering model derived from wind tunnel and full scale test data. The design of this software is described later in this paper.

### 4.3 Stability

One important function of the DCSS is to stabilise the probe as it decelerates through Mach 1. Since the probe incidence at parachute deployment, the deployment Mach number and the aerodynamics of the probe had all changed since the original analysis, the stability of the probe had to be reassessed.

The stability model used during development was created using a software package which is no longer available, so a new multi-body, 6 degree of freedom model was constructed to perform this analysis and was validated against the original model.

### 4.4 Full Entry and Descent Model

The analysis during development and the early stages of revalidation involved modelling of different stages of the Huygens sequence in isolation. This was time consuming and made it very difficult to investigate the effects of parameter changes to the overall performance of the system.

In order to investigate the effects of the new atmosphere models on the performance of the Huygens probe it was necessary to model a large number of sequences through differing atmospheres from entry interface to deployment of the main parachute to identify the most extreme conditions. To accomplish this, an existing 3 degree of freedom simulation code was extended for the purpose. The new code includes:

- Four planetary atmosphere models in addition to arbitrary look-up tables;
- Flexible sequencing based on Mach, accelerations, timing and height;
- Accurate parachute inflation models;
- The ability to model the decision logic and voting of the Huygens CDMUs; and
- The option to vary any input parameter according to statistical distributions.

The code may be used to explore the envelope of extreme values of each input parameter or to run Monte-Carlo analyses randomising the whole system.

## 5 INITIAL ASSESSMENT

### 5.1 Deployment Conditions

The five new initiation cases were used to predict descent trajectories, the deployment conditions for the parachutes and the release time for the front shield. The simulations were performed using the extreme worst case masses and aerodynamics in order to obtain the most extreme conditions at each stage. These were then used to calculate deployment times and loads for the parachutes and thence inflation loads.

The increase in range of conditions seen at mortar firing was also evident at the time of main parachute release (only 2.5 seconds later). The lowest Mach number at this time was now 1.12, which compares with 1.30 for the design sequence. The reduced Mach number gives less time for the main parachute to deploy and stabilise the probe before Mach 1, where the probe is dynamically unstable.

At the time of front shield release, 32.5 seconds after the pilot chute deployment, the range of conditions (Mach 0.34 to 0.55) still exceeds the values predicted during the development programme (Mach 0.39 to 0.51); however, they are well within the design limits (Mach < 0.6).

By the time of main parachute release, 15 minutes from pilot chute deployment, the conditions were indistinguishable from those predicted during the development programme.

The extreme limits of descent time were calculated to be 2 hours, 0 minutes and 2 hours, 31 minutes. This compares favourably with the design aim of 2 hours, 15 minutes  $\pm$  15 minutes.

### 5.2 Deployment dynamics

The pilot chute is deployed by a pyrotechnic mortar through a region of recirculating flow behind the probe. Following ejection by the mortar it first decelerates as it passes through the near wake and then accelerates towards lines taut. Too slow a deployment could result in the chute becoming caught in the wake and not deploying; too fast a deployment will increase the snatch loads at lines taut and potentially damage the parachute.

The pilot chute deployment predictions indicated the velocity at lines taut was slightly increased from the design value, giving maximum snatch forces of just under 600 N. Since the inflation load exceeds this by a factor of three, these loads are not considered to be an issue.

The main parachute is deployed by the pilot chute, which pulls the back cover away from the probe, thus deploying the parachute from its bag. The back cover / pilot chute combination and probe were designed to have a ballistic coefficient ratio of no worse than 0.7. In fact, when the new conditions and known masses are taken into account, the worst case ballistic coefficient ratio is 0.45. This indicates a very positive separation and suggests there is a possibility that the main

parachute may deploy too quickly, thus causing high snatch loads and potential searing damage to the canopy.

The deployment model was used to predict the deployment velocities and snatch loads during parachute deployment. The maximum velocity at bag strip was predicted to be 54 m/s using the new conditions, the highest velocity predicted during development was 51 m/s. Although the new velocity is higher, the difference is small enough that there is little increase in the likelihood of damage.

The peak main parachute snatch load was predicted to be a maximum of 2.7 kN, up from 2.1 kN during the DCSS design. This is much lower than the parachute design inflation load of 14.7 kN so is not a concern.

The front shield release was designed such that the worst case ballistic coefficient ratio at release was 0.7. The main source of uncertainty in this ratio during the development programme was the mass uncertainty of the front shield and probe. Since this has now been eliminated, the uncertainty in ballistic coefficient ratio has been reduced such that the predicted ratio now lies in the range 0.50 to 0.54.

It was concluded that all the component deployments and separations are robust with respect to the new conditions.

### 5.3 Stability

The reduced Mach number and increased dynamic instability at main parachute deployment leads to a possibility that the oscillations may increase during the transonic deceleration to the point that parachute bridles could become slack and wrap around other items on the probe back cover (for example the communications antennae). In order to assess the possibility, a number of simulations were carried out from the lowest expected Mach numbers with the maximum expected probe initial incidence.

Fig 3 shows the probe (heavy line) and parachute incidence when started from an initial probe incidence of 10° and parachute incidence of 2°. The parachute motion quickly damps out, while the probe oscillation is controlled quickly, reducing to less than 1° by Mach 0.7. This oscillation is well within the capabilities of the system.

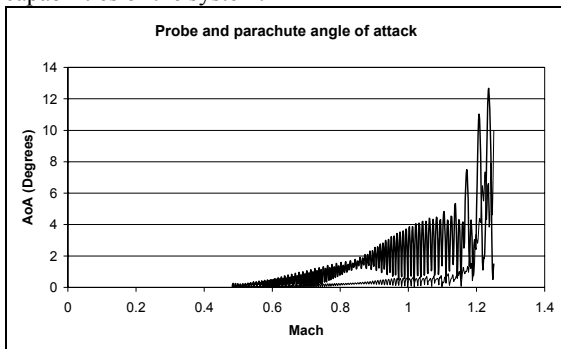


Fig. 3 Probe and Parachute incidence

The Huygens main parachute has been designed to be stable at zero incidence. However, some variants of the DGB design (including the Huygens pilot chute) tend to glide, having a non-zero stable incidence. A second simulation (fig 4) was carried out assuming the parachute had a stable incidence of 10°. This shows that the probe and parachute both start to glide with a stable incidence but the oscillation about this stable angle rapidly damps out.

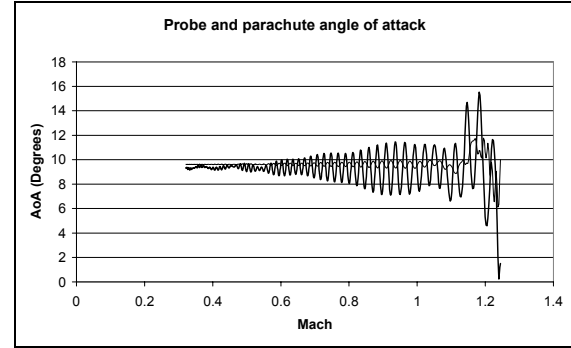


Fig 4. Unstable parachute

The stability analyses indicate that the DCSS is capable of controlling the probe as it decelerates through Mach 1 even with the new, low parachute inflation mach numbers.

## 6 INFLATION LOADS

During the DCSS development, the parachutes were tested in wind tunnels [6], in low level drop tests [7] and finally in a high altitude system drop test [8, 9]. These tests provided valuable information to assess the aerodynamic coefficients and inflation characteristics of the parachutes. During the development of the parachute for MER (a DGB of a slightly different design) a test anomaly occurred, where the opening load was significantly higher than predicted by existing models. A re-analysis of Huygens data in combination with the new MER data allowed a refinement of the opening load model.

The parachute inflation loads have been remodelled using a code that explicitly includes added mass terms. The code is based on work published in [10] which in turn is similar to the work of Cruz [11].

The fundamental equation of motion is written:

$$m_s \frac{dV}{dt} = m_s g - \frac{1}{2} \rho V^2 C_D S_p - a_{11} \frac{dV}{dt} - V \frac{da_{11}}{dt}$$

Canopy drag area evolution ( $C_D S_p$ ) was extracted from Huygens and MER test data. The added mass was defined as:

$$a_{11} = 2.136 \rho \frac{\pi D_p^3}{12}$$

Inflation time estimates were based on the Huygens test data extrapolated to the supersonic regime using Greene [12].

A typical force profile is shown in fig. 5 for the main parachute.

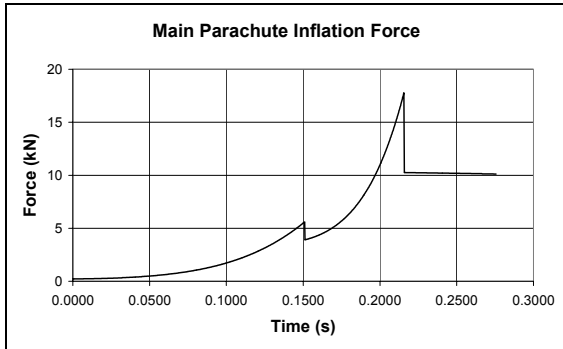


Fig. 5 – Typical parachute inflation force profile

The maximum inflation loads for the pilot and main parachutes in the worst case conditions were predicted to be 2,350 N and 17.6 kN respectively. These compare with design loads of 1,800 N and 14.7 kN.

Following the increase in predicted loads, the strength of the parachutes and probe structure were reassessed. The new loads were found to be within the structural capabilities of all components.

## 7 DETAILED ENTRY ASSESSMENT

The analyses performed during the first part of the reassessment involved analysing the performance of the descent phase of the sequence with discrete atmospheres from a very limited number of initiation conditions. This approach has two drawbacks:

- The value of each parameter which produces the worst case outcome must be correctly chosen (this is not always obvious, for instance in the case of gravity waves, and the “worst case” for one subsystem may not be the worst for another);
- Worst cases can be identified without any idea of their probability of occurrence – it is not worthwhile designing for a 1 in a million occurrence.

In order to explore the envelope of potential outcomes and determine the probability of an extreme event occurring a Monte-Carlo simulation was carried out.

### 7.1 Model

Advances in computer power over the last decade and improved software using the latest object-oriented capabilities of languages such as C++ have allowed the fidelity of entry simulations to be improved and made large Monte-Carlo runs, which would previously have required the use of supercomputers, accessible to ordinary PCs. The simulation used for the re-validation has the capability of modelling the internal logic of the

Huygens sequencer controllers as well as the inaccuracies of the sensors and uncertainty in probe parameters. The DCSS was designed using seven discrete trajectories but over 55 independent variables were available for the re-validation exercise.

### 7.2 Analysis

In order to produce a valid set of simulations it was necessary to start the simulation outside the atmosphere at an altitude of 1,270 km above the surface. This allowed specification of an initial state and 6x6 covariance matrix which produced the expected range of initial flight path angles. The software then modelled the entry and descent phases using the probe mass and aerodynamic databases.

For this analysis TitanGRAM was used in preference to the discrete models used earlier in the analysis. This produces random density and temperature profiles based on the same nominal profile used in the previous models.

Simulations were run from atmosphere interface until main parachute inflation to determine the probability of exceeding the pilot chute or main parachute inflation loads and to investigate a potential failure mode where the mortar is fired before the system is armed. A smaller number of simulations were run from atmosphere interface to landing in order to assess the potential variability in mission length.

### 7.3 Initial Conditions

The DCSS initiation points generated from the analysis are shown in fig. 6. It can be seen that the gravity wave cases used in the initial analysis (solid black line) produce initial conditions which are well outside the design range (grey lines). Two sets of Monte-Carlo results are shown: nominal sequence (crosses) and fire on arm (a single failure case – circles). These predict less extreme conditions than the worst case gravity waves but even these lie outside the design limits for the mission.

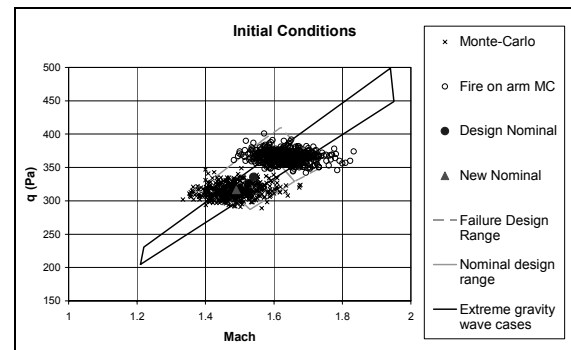


Fig. 6. DCSS Initiation Conditions

#### 7.4 Pilot Chute Inflation Loads

The pilot chute inflation force was predicted using the high fidelity inflation model within the trajectory software. Two families of inflation forces can be seen, corresponding to the fire on arm and nominal firing cases.

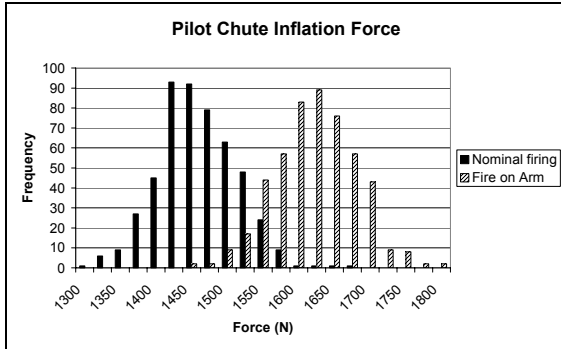


Fig. 7. Pilot Chute Inflation Force

The maximum inflation force seen during this analysis was 1800 N. This is significantly less than the value of 2334 N predicted by using all the combined worst cases.

#### 7.5 Main Parachute Inflation Loads

The main parachute is deployed 2.5 seconds after pilot chute deployment in the nominal sequence. In the fire-on-arm case this delay is increased, since the main parachute deployment time is related to the time when the pilot chute should have been deployed. The result is that the main parachute is deployed at a slightly lower Mach number and dynamic pressure than the nominal and the worst case inflation loads for the main parachute occur for the nominal sequence.

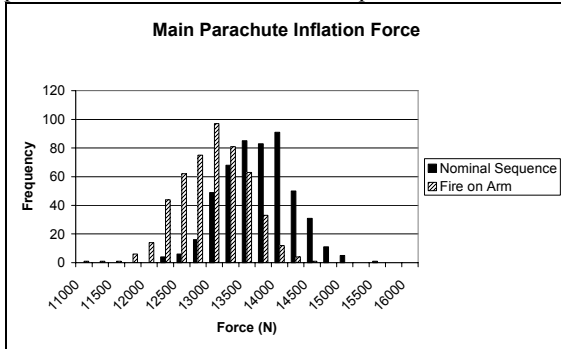


Fig 8. Main Parachute Inflation Force

Once again, the peak inflation force of 15.5 kN is much less than the value of 17.6 kN predicted using the extreme worst cases.

#### 7.6 Descent times

The overall descent time can easily be derived from the analysis. The results indicate a nominal descent time of 2 hours and 20 minutes with the  $3\sigma$  extremes lying 10 minutes either side.

## 8 DYNAMIC STABILITY

During the original development, limited testing of the dynamic stability of the probe during entry was performed in order to determine the dynamic aerodynamic coefficients ( $C_{mq}$ ). This type of testing is very expensive and it is very difficult to determine the coefficients precisely from the data. Furthermore, the flow in the base region, which largely determines the damping coefficients, is influenced by the model support. As a result the uncertainties assigned to these coefficients were large. The latest computational tools incorporating fluid/structure interaction offer the potential to determine these coefficients analytically.

Recent studies using the Arbitrary Lagrangian-Eulerian capabilities of LS-DYNA suggested that it might be possible to simulate the dynamics of the probe in a supersonic flow in order to derive  $C_{mq}$ . An Eulerian fluid mesh was created and configured with an equation of state to represent the atmospheric properties. A rigid body shell structure, free to rotate about the centre of gravity in all axes, was then created based on the probe geometry and mass properties. By prescribing a flow velocity to the fluid domain, it was then possible to simulate the flow development about the probe and any induced oscillatory motion. Extracting the angular position, rate and acceleration data then enables derivation of dynamic aerodynamic coefficients.

During development of the simulation, published test data from the Viking ballistic range tests [13] were used to verify the dynamic oscillation of the probe. The motion of this model was found to be in good agreement with the test data.

For Huygens, stability characteristics of the probe are being investigated at a range of eight Mach numbers from 0.7 to 3.0. Titan atmospheric properties with a static pressure of 200 Pa and density of  $0.0042 \text{ kg/m}^3$  are defined for the fluid domain. The simulations are initiated with the probe pitched up by  $2^\circ$  to avoid solving for a completely symmetrical case. An oscillation sequence with flow velocity vectors for the probe at Mach 1.5 is shown in Fig 9. Pressure contours at an instant in time in the same sequence is shown in Fig 10.

The initial results are encouraging and analysis is ongoing to verify performance.

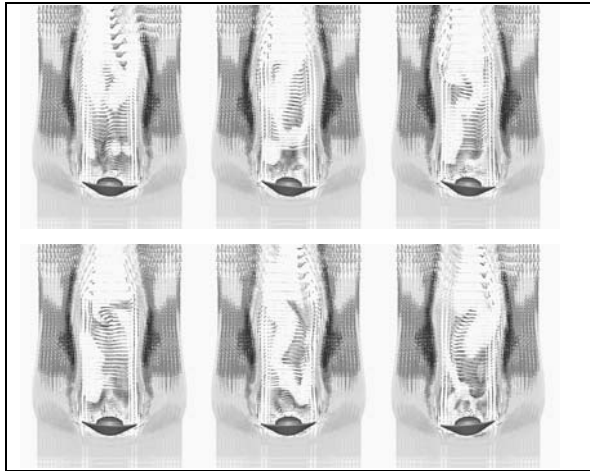


Fig 9. Mach 1.5 Oscillation Sequence

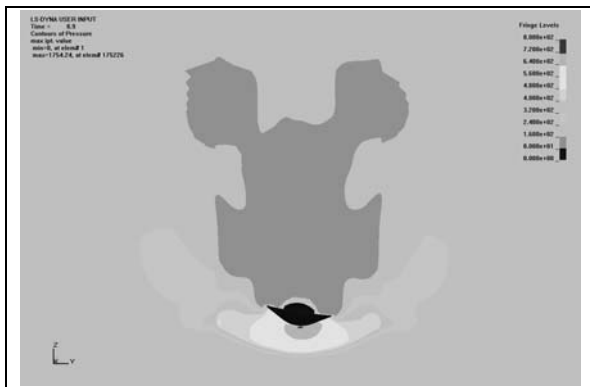


Fig 10. Mach 1.5 Pressure Contours

## 9 CONCLUSIONS

Updated analysis of the Huygens DCSS shows that it is robust with respect to the environments predicted using the latest data.

Ongoing analysis of the aerodynamic damping offers the potential to improve the analysis of entry stability.

A model has been derived which will allow the performance to be reassessed rapidly if atmosphere models are updated prior to the release of Huygens from Cassini.

## ACKNOWLEDGEMENTS

This work was funded by the European Space Agency through Alcatel Space, the Huygens prime contractor.

## REFERENCES

1. Neal, M.F. and Wellings, P.J., *Descent Control Subsystem for the Huygens Probe*, AIAA-95-1533.
2. Lellouch, E. and Hunten, D.M., *The Lellouch-Hunten Models for Titan's Atmosphere*, ESA SP-1177.

3. Yelle, R. et al., *Engineering Models for Titan's Atmosphere*, ESA SP-1177.
4. Strobel, D.F. and Sicardy, B., *Gravity Wave and Wind Shear Models*, ESA SP-1177.
5. Justus, C.G. and Duvall, A.L., *Atmospheric Models for Aerocapture*, AIAA 2004-3844.
6. Underwood, J.C. and Sinclair, R.J. *Wind Tunnel Testing of Parachutes for the Huygens Probe*, The Aeronautical Journal, October 1997.
7. Underwood, J.C., *Development Testing of Disk-Gap-Band Parachutes for the Huygens Probe*, AIAA 95-1549
8. Jäkel, E. et al., *Drop test of the Huygens Probe from a stratospheric balloon*, Advances in Space Research 21 (1998).
9. Underwood, J.C., *A System Drop Test of the Huygens Probe*, AIAA 97-1429.
10. Lingard, J.S., *The Effects of Added Mass on Parachute Inflation Force Coefficients*, AIAA 95-1561 (1995)
- 11 Cruz J.R. et al., *Opening Loads Analyses for Various Disk-Gap-Band Parachutes*, AIAA 2003-2131 (2003)
12. Greene, G.C., *Opening Distance of a Parachute*. J. Spacecraft V7 No 1 (Jan 1970)
13. Sammonds, R.I., *Transonic Static and Dynamic Stability Characteristics of Two Large-Angle Spherically Blunted High-Drag Cones*, AIAA70-564.